Influence of Injection Rate Shaping on Combustion and Emissions for a Medium Duty Diesel Engine

J. Benajes, S. Molina*, K. De Rudder
Universidad Politécnica de Valencia. CMT-Motores Térmicos, Camino de Vera, s/n 46022, Valencia, Spain
T. Rente
Chalmers University of Technology, Hörsalsvägen 7, 41296 Gothenburg, Sweden

This paper describes the effects of injection rate shaping on the combustion, fuel consumption and emission of NO_x and soot of a medium duty diesel engine. The focus is on the influence of four different injection rate shapes ; square type 1, square type 2, boot and ramp, with a variation of maximum injection pressure and start of injection (SOI). The experiments were carried out on a 1 liter single cylinder research diesel engine equipped with an amplifier-piston common rail injection system, allowing the adjustment of the injection pressure during the injection event and thus injection rate as desired. Two strategies to maintain the injected fuel mass constant were followed. One where rate shaping is applied at constant injection duration with different peak injection pressure and one strategy where rate shaping is applied at a constant peak injection pressure, but with variable injection duration. Injection rate shaping was found to have a large effect on the premixed and diffusion combustion, a significant influence on NO_x emissions and depending on the followed strategy, moderate or no influence on soot emission. Only small effects on indicated fuel consumption were found.

Key Words : Diesel, Injection Rate Shaping, Common Rail, Ignition Delay, Injection Pressure, Diesel Engine Emissions

Nomenclature

B	: A boot type of injection
CAD	: Crank Angle Degrees after top dead center
HRL	: Heat Release Law [J]
INO_X	: Emission Index of Nitrous Oxides [g_{NO}/kg_{fuel}]
IP	: Injection pressure [bar]
ISOOT	: Emission Index of soot [g_{soot}/kg_{fuel}]
Logic SOI	: The start of injection programmed in engine control unit [CAD]
R	: A ramp type of injection
Real SOI	: The real start of injection [CAD]
RoHR	: Rate of Heat Release [J/CAD]
S1	: A normal square type of injection
S2	: A modified square type of injection
SOC	: Start of Combustion [CAD]
TDC	: Top Dead Center

* Corresponding Author,
E-mail : samolina@mot.upv.es
TEL : +82-63-290-1473; **FAX** : +82-63-291-9312
Universidad Politécnica de Valencia. CMT-Motores Térmicos, Camino de Vera, s/n 46022, Valencia, Spain.
(Manuscript **Received** May 12, 2005; **Revised** June 15, 2006)

1. Introduction

Diesel engines for light and heavy duty transportation have been widely used along the last decades for their relative higher efficiency compared with the gasoline engines. Today's tightening environmental standards and user-defined needs call for both lower fuel consumption and reduced emissions. The emission legislation EURO IV, V and US 2007, which are shown in Table 1, are

Table 1 Emission legislation

Legislation	NO_x [g/kWh]	PM [g/kWh]
EURO IV	3.5	0.02
EURO V	2.0	0.02
US 2007	~0.3	~0.01

milestones for reduction of exhaust emissions of commercial diesel engines.

Consumer demands for lower fuel cost and restrictions of the emission of CO_2 have put additional pressure on improving engine efficiency, which is unfortunately conflicting with the measures for emission reduction. Present injection and air management systems are in general incapable of achieving by themselves the stringent emissions limits, including here CO_2, which is proportional to the fuel consumption. Therefore, additional measures are required for reducing pollutant emissions. Often, the combination of a combined increase in EGR rate and injection pressure is described as a way to meet reduce emissions.

The effect of injection pressure on fuel spray formation and combustion has been well described by Payri et al.(2005), Jeongkuk et al.(2004) and Kyu Keun et al.(2005). However, not only the average injection pressure is important, but also the instantaneous injection pressure or injection rate, as was described by Jinwook and Kyoungdoug (2005), and Jinwook (2006). They reported that it is possible to influence the injection rate slope by altering the control signal of a common rail injector; this influences the spray formation, combustion and ultimately the emissions.

Injection rate shaping is an extension of this principle and it is a very promising approach to reduce engine emissions. Usually the aim of modulation the fuel injection rate in a DI diesel engine is to reduce the mass flow rate at the start of the injection event. This action reduces the amount of fuel that is mixed with air and burnt during this early phase. Consequently, there is a lower heat release rate, and lower local temperatures, leading to lower NO_x emissions (Heywood, 1988). This conjecture has been explored (Beck and Chen, 2000), by means of restricting the opening motion of the needle in a unit injector, and thus producing a boot injection. Reported results with this strategy show a reduction in NO_x of about 50% with an increase of only 1% in BSFC, despite a significant increase in combustion time from 26 to 42 crank angle degrees.

Juneja et al.(2004) used KIVA simulations to demonstrate that injection rate shapeing stronly affects the fuel spray properties and the formation and reduction of contaminants such as soot and NO_x.

Erlach et al.(1995), achieved flexible injection rates by means of a modified unit injector with two solenoid valves. At a constant value of BSFC and soot, a short boot reduced NO_x emissions by 14%. A long boot injection shape achieved a reduction in NO_x and BSFC of 9% and 7% respectively, comparing points of equal soot, and taking the plain injection rate shape as a reference.

Similar results were obtained in the study presented by Kato et al.(1998). When the initial injection rate is reduced by restricting the needle lift, at a constant value of NO_x, the premixed combustion is inhibited and the injection timing could possibly be advanced. As a result, fuel consumption improved but black smoke emission increased due to the rate shaping.

Kohketsu et al.(2000) combined two independent common rail systems working at two different pressures with a switching valve selecting the pressure sent to the injector. The noticeable results were a decrease in fuel consumption and soot at constant NO_x with respect to a conventional common rail system at medium speed and high load mode.

Injection rate shape can also be modulated with the use of different cams in the injection pump as described by Ishiwate et al.(1994) with a concave and tangential cam in a pump-line-nozzle system at medium engine speed. Their results showed that the concave cam (which produces a lower initial injection rate and almost a boot injection) causes an increase in PM at high load, while at medium load there are simultaneous reductions in NO_x and PM with a slight increase in BSFC.

The advantages of avoiding the natural steep

injection rate of common rail systems have also been explored. A slow increase in injection rate was attained by Nehmer and Reitz (1994), by changing the valve within the common-rail injector. Reported results show that a slow injection rate rise has a small penalty in the NO_x-particulate trade-off. However, in this case it was possible for combustion to continue longer into the cycle with lower soot levels than those with faster injection rate tests.

A similar study was described by Schwarz et al. (1999), comparing the advantages of a ramp type injection which is natural in PLN systems with respect to the rectangular injection rate. In the important operating range of heavy-duty diesel engines at high load and low speed, the slow initial injection process is able to induce low combustion temperatures, while the high injection pressure at the end of the relatively long injection time favours soot oxidation. The reported consequence is lower NO_x with a ramp injection rate, and similar soot emissions and BSFC to those found when using the rectangular injection shape.

It can therefore be concluded that depending on the injection system, different results can be obtained when using boot injections. Moreover, depending on the load and speed of the engine, the rate shaping mechanisms can be more or less efficient.

2. Experimental Facility and Methodology

The engine used is a single cylinder research engine, based on a commercial medium duty diesel engine. The cylinder displacement is 1.02 l, the bore/stroke relation 0.82 and a compression ratio of 17.15. The injector is a Bosch common rail injection with 8 orifices of 166 μm diameter. The injection system was the Bosch APCRS (Amplifier Piston Common Rail System), see Fig. 1. This system was developed as a new generation of common rail systems for heavy duty application. This common rail system works with a relative low rail pressure (300 to 800 bar). The fuel pressure is amplified for the duration of the injection event with a hydraulic piston, up to 2.8 times of the rail

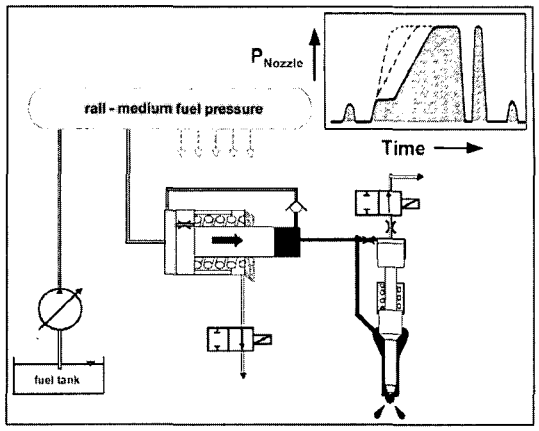

Fig. 1 Amplifier piston common rail system

pressure. The amplifier and injector (normal common rail injector) are electronically controlled. This combination results in a highly flexible injection system in the field of injection rate shaping. The maximum achievable injection pressure is around 2000 bar, however, for durability reasons the maximum pressure was limited to 1600 bar. Injection pressure was measured by a piezoelectric pressure transducer in the high pressure line, just before the common rail injector.

The actual evolution of the fuel introduction rate into the combustion chamber cannot be measured online during the engine tests. Instead, the injection rate was measured off-line in a so-called injection discharge-rate-curve indicator (EVI-IAV). In this system, the injection process is carried out in a specific measuring tube filled with fuel. The discharge of the fuel produces an increase in pressure that is proportional to the fuel mass increase Instantaneous pressure in the fuel tube is recorded and later instantaneous mass flow rate is computed based on average fuel flow and taking into account fuel temperature. (Bosch, 1966; Arcoumanis and Baniasad 1993).

The research engine was installed in a fully instrumented test cell, with all auxiliary facilities required for the operation and control of the engine. Fig. 2 shows a scheme of the installation. To provide the intake air conditions as in the real production engine, a screw compressor supplied the required boost pressure, while air temperature and humidity at the engine intake was controlled

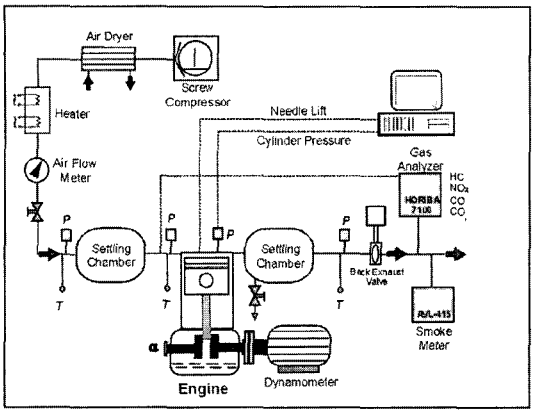

Fig. 2 Experimental set-up

by an external cooler and dryer, keeping the desired inlet conditions in a settling chamber upstream of the intake pipe. Air flow rate was measured by a volumetric flow meter. The exhaust back pressure produced by the turbine in the multi cylinder engine was reproduced by a throttle in the exhaust system, controlling the pressure in the exhaust settling chamber.

The in-cylinder pressure was measured with a piezoelectric pressure transducer. Pressure traces for 25 engine cycles were recorded in order to compensate for the statistical dispersion in engine operation. The filtered average pressure signal was used as input for a combustion diagnostic model.

The NO_x, CO, HC, CO_2, and O_2 measurements were performed with a HORIBA 7100 analyzer. Smoke emission was measured with a variable sampling smoke meter, providing results directly in filter smoke number that were transformed into dry soot mass emissions by means of the correlation proposed by Christian et al.(1993).

From the engine tests, direct information on performance behavior can be obtained in terms of brake specific fuel consumption (BSFC) and pollutant emissions, mainly NO_x and Dry Soot. Valuable additional information can be extracted from in-cylinder pressure, such as the heat release law (HRL) and several associated parameters, namely combustion duration, burnt temperature, ignition delay, etc. The combustion diagnosis code CALMEC (Lapuerta et al., 1999 ; 2000) has been used for this purpose ; it is based on the solution of the energy equation inside the cylinder, with the assumption of uniform pressure and temperature over the volume. This single-zone model approach allows calculation of the instantaneous average temperature as well as the instantaneous heat release from the burnt fuel. With simple additional hypotheses (Desantes et al., 2000 ; Garcia et al., 2000 ; Ishida et al., 1996), the single zone model can be extended to a two-zone model that provides information on the instantaneous temperature of both the burnt and unburnt gas fractions.

3. Injection Strategies

Engine mode — One basic engine operating mode has been chosen, corresponding to the A75 of the European Stationary Cycle (ESC). This engine mode corresponds to a speed of 1550 rpm, the injected fuel mass was maintained constant at 80 mg/stroke, while maintaining the intake and exhaust pressure constant at respectively 2.00 and 2.10 bar. The intake temperature was 36℃.

Injection strategies — For the tested mode, 4 different injection rate shapes were tested, named square type 1 (S1), square type 2 (S2), ramp (R) and boot (B). These injection rate shapes were tested at 4 different maximum pressure levels : at 900, 1100, 1300 and 1600 bar. Fig. 3 shows a scheme of the injection rates shapes of all these strategies. The goal of all these tests is to separate the effect of injection rate shape, injection pressure, and injection duration. All strategies were tested for logic SOI varying between −10 to +2 CAD ATDC in steps of 2 CAD.

A detailed injection rate shape comparison is shown in Fig. 4. In this figure, four injection strategies with constant injection duration are depicted, these are the injection rate shapes marked with a "*" in Fig. 3.

With the proposed strategy of Fig. 3, the effect of injection rate shaping is investigated in two ways. Firstly, different injection rate shapes are compared at equal maximum injection pressure (vertical comparison in Fig. 3). And secondly, different injection rate shapes are compared for constant injection duration (diagonal comparison in Figs. 3 and 4).

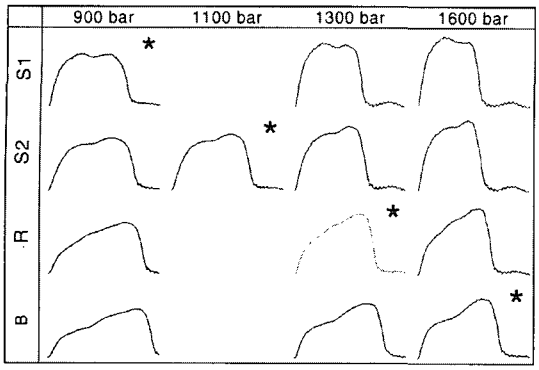

Fig. 3 Injection rate shape for the tested injection strategies (*constant injection duration)

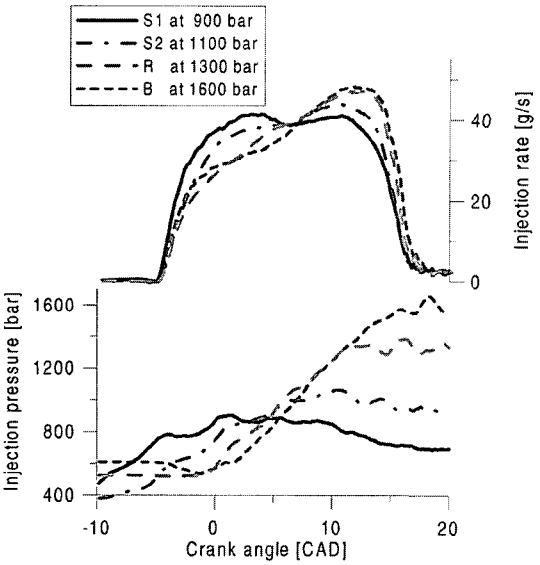

Fig. 4 Four different injection rate shapes with constant injection duration

4. Combustion Analysis

4.1 Ignition delay phase

The ignition delay is defined as the time between the start of injection (Real SOI) and start of combustion (SOC) (see Fig. 5). The real SOI is the start of fuel introduction into the combustion chamber (this is derived from the measurements of the injection discharge-rate-curve indicator); whereas the Logic SOI is the crank angle programmed in the electronic control unit of the injection system. The definition of the SOC is defined here as the moment when the rate of heat

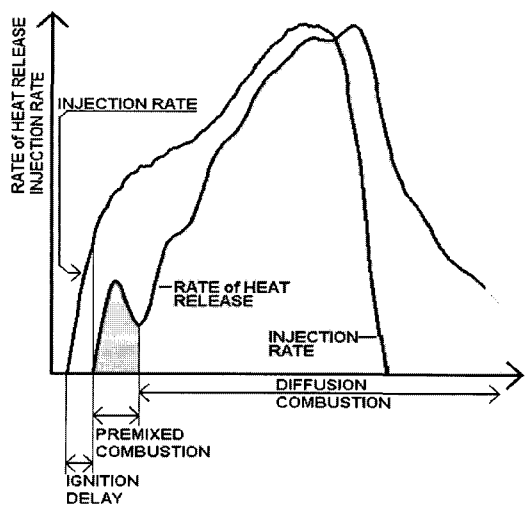

Fig. 5 Ignition delay, premixed combustion (Boot at 1600 bar)

release is changing from negative to positive. The actual combustion starts earlier, but the released energy is lower than the energy required to evaporate the injected fuel. During the auto-ignition delay period several chemical and physical processes take place. The physical processes can be separated into the atomization of the liquid fuel jet, the evaporation of the fuel droplets and the mixing of the fuel vapor with air. The fuel atomization depends on the injection pressure, orifice diameter, fuel viscosity, and in-cylinder pressure at the time of injection. The fuel evaporation depends on the droplet size, droplet distribution and velocity, in-cylinder temperature and pressure. The fuel/air mixing is mainly controlled by the injector and combustion chamber design. The chemical processes are pre-combustion reactions of the fuel, air, residual gas mixture. The chemical reaction rate is mainly dependent on the temperature (Baert et al., 1999 ; Rosseel and Sierens, 1996).

Influence of injection rate shape at constant injection duration — The effect of injection rate shaping at constant injection duration on the ignition delay, injection pressure and injection rate is shown in Fig. 6 for all tested injection rate shapes at the same logic SOI of −8 CAD. For each rate shape, the injection pressure and rate is depicted versus the crank angle, from the start of injection until the start of combustion (=auto-

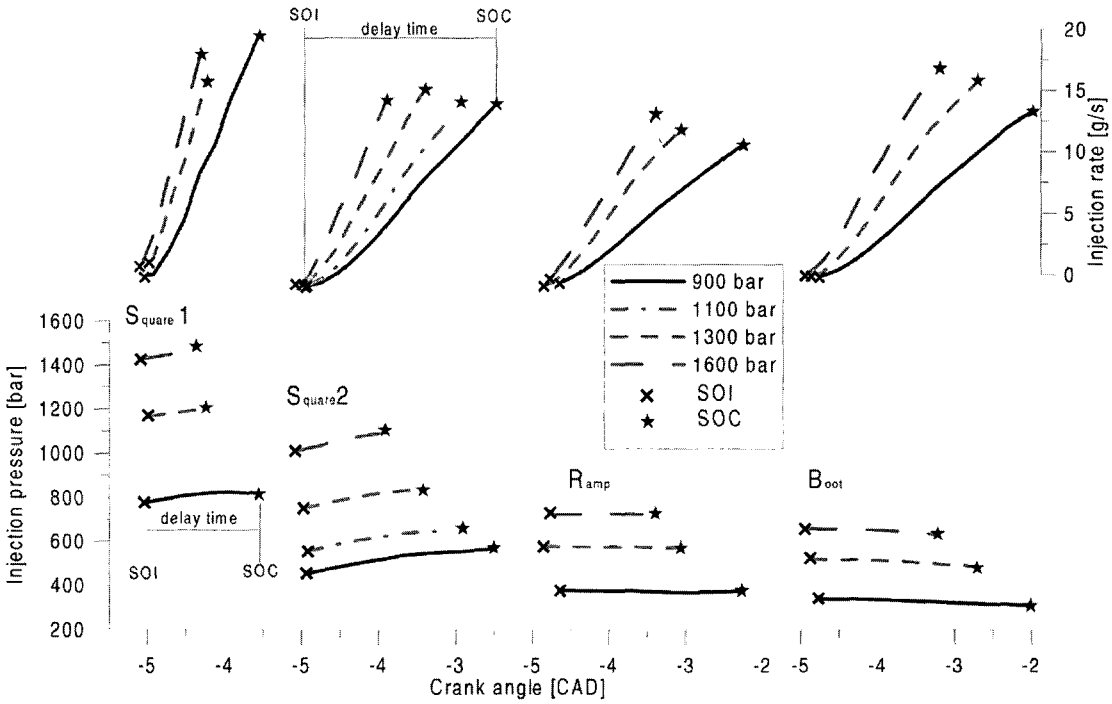

Fig. 6 Injection rate and injection pressure, during the ignition delay time for logic SOI −8 CAD ATDC

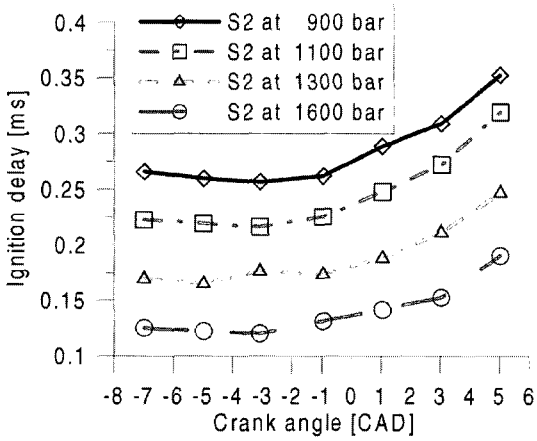

Fig. 7 Delay time for different maximum injection pressures of the injection rate square type 2

ignition delay).

Figure 6 shows that a square type 1 rate shape with a maximum injection pressure of 900 bar has an injection pressure of 800 bar during the auto-ignition delay ; a boot rate shape with a maximum injection pressure of 1600 bar has a similar injection pressure of 700 bar during the auto-ignition delay. It is known that an increase in injection pressure enhances fuel atomization and the fuel/air mixing process (Heywood, 1988 ; Kobori et al., 2000), resulting in a reduction of the physical delay time and thus shorter auto-ignition delay period. This effect explains the small reduction of the auto-ignition delay depending on the chosen injection strategy, see Figs. 6 and 7.

Influence of injection rate shape at constant injection pressure - Fig. 6 shows that when a maximum injection pressure of 1600 bar is maintained, the injection pressure during the auto-ignition delay depends on the chosen rate shape. The auto-ignition delay times varies depending on the injection pressure during the auto-ignition delay time. Thus the auto-ignition delay depends on the chosen injection rate shape.

Figure 7 shows the well known effect of increasing injection pressure vs SOI on the auto-ignition delay time. The auto-ignition delay time increases for later SOI due to reduced in-cylinder temperature and thus lower chemical reaction rate. This behavior was not only seen for the square type 2 shape, but for all tested rate shapes. The auto-ignition delay reduces for increasing

injection pressure.

4.2 Premixed combustion phase

The premixed combustion phase is generally seen as the phase when the fuel that has been mixed with air during the auto-ignition delay period, is burned (Heywood, 1988). Usually, this fuel burns very fast, leading to a rapid increase of released heat; indicated by a peak in the rate of heat release curve, see also Fig. 5.

Influence of injection rate shape at constant injection duration — When rate shaping is applied at constant injection duration, all rate shapes show a similar duration of the premixed combustion. However, the lowest amount of fuel is burnt in premixed mode for a boot and ramp injection rate shape (see Table 2).

Influence of injection rate shape at constant injection pressure — When rate shaping is introduced at a equal maximum peak injection pressure, it can be seen in Table 2 that a boot and ramp shape have a longer premixed combustion than a square injection rate shape. Also the fuel that is burnt in premix mode (see also definition in Fig. 5), is reduced for ramp and boot in comparison with a square type. This can be explained by the rate of injection during the ignition delay and premix burn period (see Fig. 9). A boot and ramp shape show a similar injection rate at the first instants of injection, thus the premixed combustion phase is very similar. Both square shapes show a higher rate of injection during the premixed combustion, this explains a shorter but more intense premix combustion.

4.3 Mixing-controlled combustion phase

The mixing-controlled combustion phase follows the premixed combustion. In this phase, the burning rate is primary controlled by the mixing rate between the fuel vapor and the air (Heywood, 1988).

Influence of injection rate shape at constant injection duration — The strategy was chosen to keep the injected fuel mass per cycle and the injection duration constant, resulting in higher maximum injection pressures when the square type was changed to a boot type (see Fig. 3). Therefore these two effects, changed rate shape and changed injection pressure, are influencing the results. The effects on the rate of heat release curve are shown in Fig. 8, for a SOI at −8 CAD ATDC. It can be observed that if the main part of the fuel is injected later and at a higher pressure (boot type), the peak of the mixing-controlled combustion phase is shifted towards later crank angles. Comparing square type 1 at 900 bar with the boot type at 1600 bar, it can be seen that the injection rate for square type 1 at 900 bar is higher at the beginning of the injection (Fig. 6). This increased injection rate is known to improve the mixing process, thus resulting in an earlier more intense combustion. In the case of a boot rate shape at a peak pressure of 1600 bar the main part is injected at the end of the injection period when the ambient conditions in the combustion chamber are less favorable for the combustion process, because the in-cylinder temperature and pressure are decreasing due to the downwards movement of the piston, resulting in a longer combustion duration.

Table 2 Ignition delay and premixed combustion

Shape	IP max [bar]	Inj. Duration [ms]	Ignition delay [ms]	Premixed combustion [ms]	Fuel burnt in premix [mg]
S1	1600	1.84	0.08	0.30	43
S2		1.84	0.08	0.30	43
R		1.84	0.08	0.30	43
B		1.84	0.08	0.30	43
S1	900	±2.38	0.08	0.30	43
S2	1100		0.08	0.30	43
R	1300		0.08	0.30	43
B	1600		0.08	0.30	43

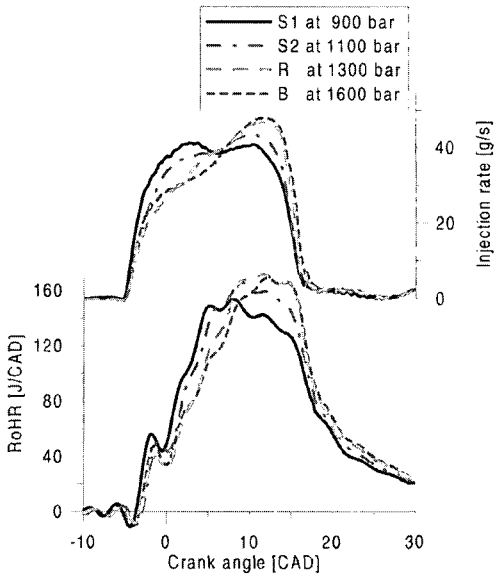

	B 1600	R 1300	S 2 1100	S 1 900
SNO_x [g/kWh]	11.5	11.9	13.1	14.5
INO_x [g/kg]	49.1	51.8	56.5	65.0

Fig. 8 Effect of rate shaping at constant injection duration on combustion and emissions for SOI −8 CAD ATDC

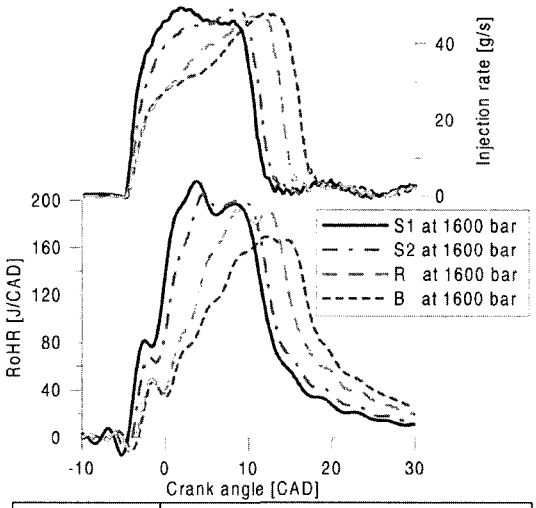

	S1 at 1600 bar	S2 at 1600 bar	R at 1600 bar	B at 1600 bar
SNO_x [g/kWh]	23.7	21.0	14.8	11.5
INO_x [g/kg]	105.7	93.1	64.0	49.1

Fig. 9 Effect of rate shaping at a constant maximum injection pressure of 1600 bar and SOI −8 CAD ATDC

Influence of injection rate shape at constant injection pressure — This strategy keeps the injected fuel mass per cycle and the peak injection pressure constant, resulting in longer injection duration when the square type was changed to a boot type (see Fig. 3). Therefore these two effects, changed rate shape and changed injection duration, are influencing the results. The cylinder pressure and rate of heat release curves for changing injection rate shapes at a maximum injection pressure of 1600 bar shown in Fig. 9. One can see that a high injection rate at the first part of the injection event leads to a high rate of heat release. One explaining factor is the advanced combustion process, since increased injection pressure is known to shorten the ignition delay time for the same SOI (see Fig. 6). Further, higher injection pressure provides more turbulent kinetic energy resulting in improved fuel/air mixing and a higher burning rate. This combined with more fuel injected earlier in the combustion leads to lower fuel consumption. In the case of a boot type most fuel is injected later at lower cylinder temperature and pressure, resulting in a lower burning rate and thus longer combustion duration.

4.4 Fuel efficiency

From the cylinder pressure trace, the indicated mean effective pressure and indicated power was calculated. Based on this calculation, the fuel consumption can be expressed as indicated fuel consumption.

Influence of injection rate shape at constant injection duration — Table 3 shows that all values for indicated fuel consumption are similar when injection rate shapes are compared at constant injection duration. However, a square injection rate shape seems to show a lower indicated fuel consumption than a boot injection. The absolute difference is due, on one hand, to the center of combustion of the different shapes, with optimum values around the TDC. On the other hand, at the same logic SOI, small variations in the actual SOI can appear between injection rates, due to the hydraulic behavior of the system. It can be seen that for increasing injection pressure, the indicated fuel consumption of ramp and boot improves,

Table 3 Analysis of indicated fuel consumption for SOI −8 CAD ATDC

S1	900	−5.04	188.2
S2		−4.93	188.9
R		−4.65	197.7
B		−4.76	204.6
S2	1100	−4.93	188.2
S1	1300	−4.87	188.1
S2		−4.98	188.0
R		−4.85	190.5
B		−4.87	196.3
S1	1600	−5.15	189.2
S2		−5.07	188.0
R		−4.77	190.9
B		−4.94	191.4

while the indicated fuel consumption for the square types remains constant.

Influence of injection rate shape at constant injection pressure — In Table 3 can be seen that changing from a square type of injection to a boot type of injection at constant IP, will always worsen the fuel consumption for the same reasons as mentioned before. However at higher injection pressures this fuel consumption increase is lower.

5. Pollutant Emissions

5.1 NO_x emissions

Influence of injection rate shape at constant injection duration — The effect of different injection rates with constant injection duration on NO_x emissions is shown in Fig. 10. The corresponding injection rates can be found in Fig. 8. In the case that the injection rate is lower at the beginning of the injection, the NO_x emissions are lower. Thus, a boot shape with a maximum pressure of 1600 bar resulted in lower NO_x emissions than a square type 1 shape with a maximum injection pressure of 900 bar, even though that both have the same injection duration. Fig. 8 shows a comparison of the rate of heat release for injection rate shapes : boot at 1600 bar and square type 1 at 900 bar. The rate of heat release of square type 1 at 900 bar is higher then that of boot at 1600 bar during the first part of the diffusion combustion, when in-cylinder pressure is still high. This results in a slightly higher burnt temperature as can be seen in Fig. 11.

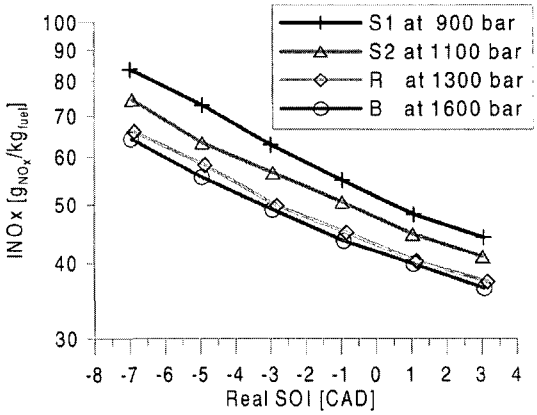

Fig. 10 INO_x dependency for constant injection duration vs SOI

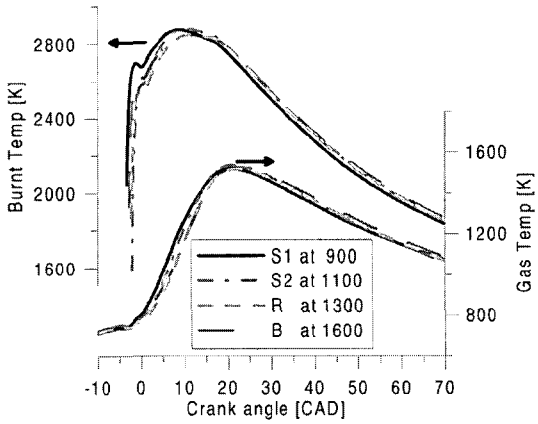

Fig. 11 Burnt and gas temperature for injection rate shapes with a constant injection duration at a SOI of −8 CAD ATDC

According to the extended Zeldovich mechanism, the formation rate of NO_x increases exponentially to the local flame temperature and to a lesser extent, reduces for reducing local oxygen concentrations (Lavoie et al., 1970). The boot type of injection rate shape in Fig. 11 shows a lower peak in burnt gas temperatures and this peaks occurs later, when the local oxygen concentration is reduced due to combustion of previous injected fuel. This can explain that despite the small difference in burnt gas temperature, large differences are found in the NO_x emissions. As a result of this, the square type 1 injection rate shape at 900

emits the highest and a boot rate shape at 1600 bar lowest amount of NO_x.

Influence of injection rate shape at constant injection pressure — In Fig. 12 it can be seen that despite an equal maximum injection pressure, a boot type of injection rate shape produce much lower NO_x emissions than a square type of injection rate shape. The maximum injection pressure is reached later in the injection event in case of a boot type of rate shape (see Fig. 9). This explains the lower and the later peak in burnt gas temperatures in Fig. 13, in the case of a boot rate shape. The formation rate of NO_x increases exponentially with the temperature, thus the lower peak in burnt gas temperatures typical for a boot injection leads to lower NO_x emissions.

It was found that an advanced SOI resulted in higher NO_x emissions for all injection strategies studied. For the range of SOI tested, an earlier SOI shifts the combustion closer to TDC (Figs. 10 and 12). When fuel is burnt close to TDC, the gas temperature is increased due to the compression of the burnt gases (Ahmad and Plee, 1983). It was found that the peak of the burnt gas and gas temperature are increased for advanced injection timing. The well known Zeldovich mechanism states that the formation rate of NO_x increases exponentially with the temperature, thus the higher burnt gas temperatures, typical for advanced SOI, leads to an increase in NO_x emissions.

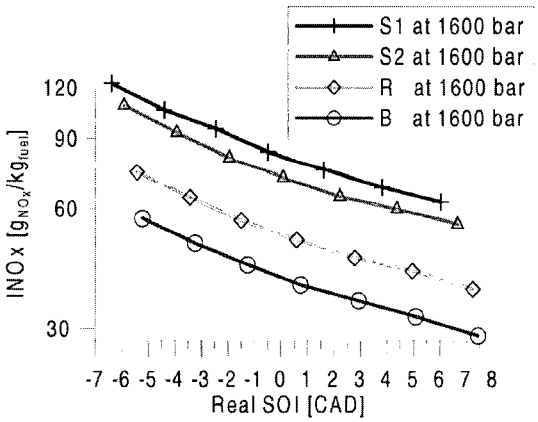

Fig. 12 INO_x emissions for a maximum injection pressure of 1600 bar vs SOI

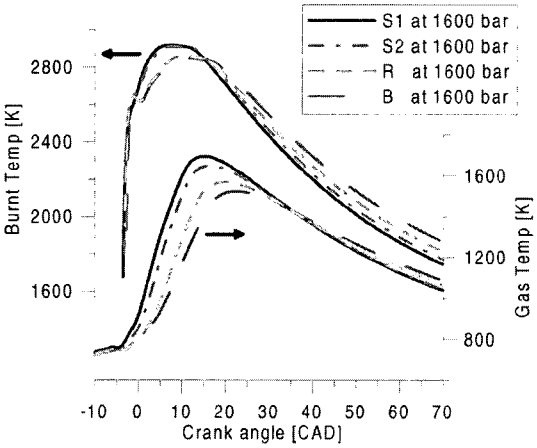

Fig. 13 Burnt and gas temperature for a maximum injection pressure of 1600 bar at a SOI of −8 CAD ATDC

5.2 Dry soot emissions

Influence of injection rate shape at constant injection duration — To investigate the effect of rate shaping at constant maximum injection pressure on soot emissions, the peak injection pressure was increased from 900 to 1600 bar, while the rate shape was changed from a square to a boot type. The dry soot emissions are shown in Fig. 14 for all tested SOI. The obtained soot values are very low, with a maximum of 0.029 g_{soot}/kg_{fuel} which corresponds to 0.06 FSN, this is at the lower border of what can be measured. Because of these low soot levels, only limited conclusions can be made.

Changing a square type of injection rate shape with an IP of 900 bar for a boot type of rate shape

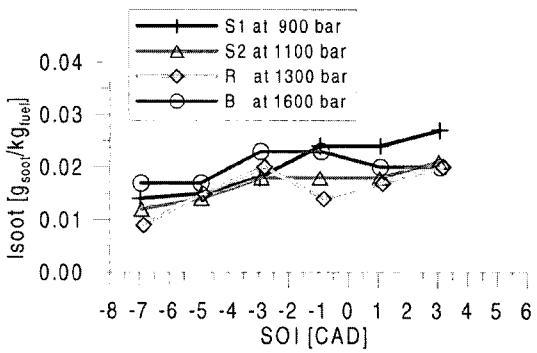

Fig. 14 Indicated soot emissions for rate shapes with constant injection duration

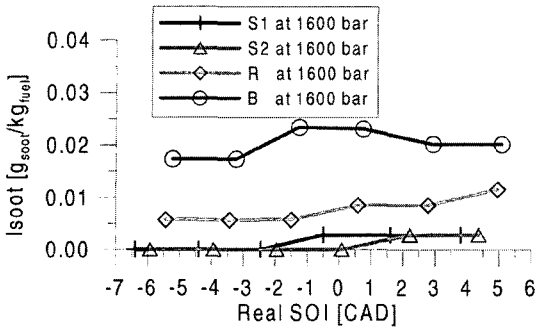

Fig. 15 Indicated soot emissions for rate shapes with a maximum injection pressure of 1600 bar

at an IP of 1600 bar, has a very small effect on the soot emission.

Influence of injection rate shape at constant maximum injection pressure — When different injection rate shapes are tested at the same maximum injection pressure (1600 bar), the differences in soot emissions are larger (as can be seen in Fig. 15) compared to the case described in previous paragraph. The absolute soot emissions are even lower.

The final concentration of soot emissions is a result of two processes acting against each other: soot formation and soot oxidation. At the first part of the injection event, a boot type has a lower injection pressure, leading to a reduced flame lift-off length, and therefore also a reduced amount of air entrained into the spray, increasing the soot formation compared to a square type (Chomiak and Karlsson, 1996). Also in Fig. 13, it can be seen that the burnt gas temperature of a boot injection stays longer in the window of 1800-2600°K compared to a square type of injection, this temperature window is the soot formation area (Kazuhiro and Uoshiki, 2001).

When a square type of injection is replaced with a boot type of injection rate shape with the same peak injection pressure, the soot emission increases but is still at a very low level.

6. Conclusions

In this article, rate shaping was evaluated on its influence on the combustion process and the influence on fuel consumption and emissions as NO_x and soot. Four different rate shapes were compared: a classic common rail square type, a modified square type, a ramp and a boot type, all rate shapes were investigated at peak injection pressures from 900 to 1600 bar. The influence of these rate shapes was studied at constant maximum injection pressure, and at constant injection duration for different start of injections.

Influence of injection rate shape at constant injection duration — It was found that when a square type of injection rate shape is changed to a boot type at constant injection duration, the peak injection pressure has to be increased from 900 to 1600 bar. The auto-ignition delay and premixed combustion show only small changes because the injection pressure during this period is at a similar level in all cases. The mixing controlled combustion phase is characterized by a later and lower peak in the rate of heat release, the average and burnt gas temperatures are slightly reduced. The fuel-indicated NO_x emission reduces by 26% with a 1.7% penalty in indicated fuel consumption at an approximated constant fuel-indicated dry soot emission.

Influence of injection rate shape at constant maximum injection pressure — When the injection rate shape was changed from a square to a boot type at a peak injection pressure of 1600 bar, the injection duration has to be increased. The injection pressure during the auto-ignition delay is reduced, and the auto-ignition delay and premixed combustion time increase, however less fuel is burnt in premixed combustion. The mixing controlled combustion duration is increased and the burning rate is reduced, the average and burnt gas temperatures show a significant reduction. The fuel-indicated NO_x emission reduces with 51% while the fuel penalty is 1.1%, the dry soot emission changes from too low to measure to around 0.02 $g_{dry\ soot}/kg_{fuel}$.

Acknowledgements

This study has been carried out in the frame of EU project CRICE in the 'competitive and sustainable growth' program. The authors wish to express their gratitude to the European Commu-

nity for supporting the research and to the partners of this project for their collaboration.

The participation of Ms. T. Rente was supported through the European Community Marie Curie Fellowship.

References

Ahmad, T. and Plee, S. L., 1983, "Application of Flame Temperature Correlations to Emissions from a Direct-Injection Diesel Engine," *SAE paper*, No. 831734.

Arcoumanis, C. and Baniasad, M.S., 1993, "Analysis of Consecutive Fuel Injection Rate Signals Obtained by the Zeuch anD Bosch Methods," *SAE paper*, Np. 930921.

Baert, R. S. G., Beckman, D. E. and Veen, A., 1999, "Efficient EGR Technology for Future HD Diesel Engine Emission Targets," *SAE Paper*, No. 1999-01-0837.

Beck, N. J. and Chen, S. K, 2000, "Injection Rate Shaping and High Speed Combustion Analysis — New Tools for Diesel Engine Combustion Development," *SAE paper*, No. 2000-01-0705.

Bosch, W., 1966, "The Fuel Rate Indicator : A new Measuring Instrument for Display of the Characteristics of Individual Injection," *SAE paper*, No. 660749.

Chomiak, J. and Karlsson, A., 1996, "Flame Liftoff in Diesel Sprays," *Twenty-Sixth Symposium (International) on Combustion/The Combustion Institute*, pp. 2557～2564.

Christian, R., Knopf, F., Jasmek, A. and Schindler, W., 1993, "A New Method for the Filter Smoke Number Measurement with Improved Sensitivity," (in German), *MTZ 54*, pp. 16～22.

Desantes, J. M., Arrégle, J., Molina, S., 2000, "Influence of the EGR Rate, Oxygen Concentration and Equivalent Fuel/Air Ratio on the Combustion Behaviour and Pollutant Emissions of a Heavy Duty Diesel Engine," *SAE Paper*, No. 2000-01-1813.

Erlach, H. et al., 1995, "Pressure Modulated Injection and its Effect on Combustion and Emissions of a HD Diesel Engine," *SAE paper*, No. 952059.

García, J., Gil, A. and Estellés, V., 2000, "Theoretical and Experimental Model for the Burnt Products of Combustion Temperature Calculating on Direct Injection Diesel Engines," (in Spanish), *XIV Congreso Nacional de Ingeniería Mecánica, Anales de Ingeniería Mecánica*, Año 13, Vol. 2, pp. 2023～2028.

Heywood, J. B., 1988, *Internal Combustion Engine Fundamentals*, McGraw-Hill, New York.

Ishida, M., Ueki, H., Matsumura, N., Yamaguchi, M. and Luo, G. F., 1996, "Diesel Combustion Analysis Based on Two Zone Model (Comparison Between Model Analysis and Experiment)," *JSME* Int. Journal, Series B, Vol. 39, No. 1, pp.185～192.

Ishiwate, H. et al., 1994, "Recent Progress in Rate Shaping Technology for Diesel In-line Pumps," *SAE paper*, No. 940194.

Jeongkuk, Y. et al., 2004, "A Study on the Behavior of Evaporating Diesel Spray Using LIEF Measurement and KIVA code," *KSME I. J.*, Vol. 18, No. 12, pp. 2303～2309.

Jinwook, L. and Kyoungdoug, M., 2005, "Effects of Needle Response on Spray Characteristics in High Pressure Injector Driven by Piezo Actuator for Common-Rail Injection System," *KSME I. J.*, Vol. 19, No. 5, pp. 1194～1205.

Jinwook, L., Kyoungdoug, M., Kernyong, K. and Choongsik, B., 2006, "Hydraulic Simulation and Experimental Analysis of Needle Response and Controlled Injection Rate Shape Characteristics in a Piezo-Driven Diesel Injector," *SAE paper*, No. 2006-01-1119.

Juneja, H., Ra, Y. and Reitz, R. D., 2004, "Optimization of Injection Rate Shape Using Active Control of Fuel Injection," *SAE paper*, No. 2004-01-0530.

Kato, T. et al., 1998, "Common Rail Fuel Injection System for Improvement of Engine Performance on Heavy-Duty Diesel Engine," *SAE paper*, No. 980806.

Kazuhiro, A. and Uoshiki T., 2001, "Mechanism of the Smokeless Rich Diesel Combustion by Reducing Temperature," *SAE paper*, No. 2001-01-0655.

Kobori, S., Kamimoto, T. and Aradi, A., 2000, "A Study of Ignition Delay of Diesel Fuel Sprays," *Int.J. Engine Research*, Vol. 1, No. 1, pp. 29～39.

Kohketsu, S., Tanabe, K. and Mori, K., 2000, "Flexibly Controlled Injection Rate Shape with Next Generation Common Rail System for Heavy-Duty DI Desel Engines," *SAE paper*, No. 2000-01-0705.

Kyu Keun, S., Sang Cherl, S. and Jang Heon, K., 2005, "Effect of the Injection Parameters on Diesel Spray Characteristics," *KSME I. J.*, Vol. 19, No. 6, pp. 1321~1328.

Lapuerta, M., Armas, O. and Bermúdez, V., 2000, "Sensitivity of Diesel Engine Thermodynamic Cycle Calculation to Measurement Errors and Estimated Parameters," *Applied Thermal Engineering*, Vol. 20, No. 9, pp. 843~861.

Lapuerta, M., Armas, O. and Hernúndez, J. J., 1999, "Diagnostic of D. I. Diesel Combustion from In-Cylinder Pressure Signal by Estimation of Mean Thermodynamic Properties of the Gas," *Applied Thermal Engineering*, Vol. 5, pp. 513~519.

Lavoie, G., Heywood, J. and Keck, J., 1970, "Experimental and Theoretical Study of Nitric Oxide Formation in Internal Combustion Engines," Combusion Science and Technology, Vol. 1, pp. 313~326.

Nehmer, D. A. and Reitz, R. D., 1994, "Measurement of the Effect of Injection Rate and Split Injections on Diesel Engine Soot and NO_X Emissions," *SAE paper*, No. 940668.

Payri, R., Salvador, F. J., Gimeno, J. and Soare, V., 2005, "Determination of Diesel Sprays Characteristics in Real Engine in-Cylinder Air Density and Pressure Conditions," *KSME I. J.*, Vol. 19, No. 11, pp. 2040~2052.

Pierpont, D. A., Montgomery, D. T. and Reitz, R.D., 1995, "Reducing Particulate and NO_x Using Multiple Injections and EGR in a D. I. Diesel," *SAE Paper*, No. 950217.

Rosseel, E. and Sierens, R., 1996, "The Physical and the Chemical Part of the Ignition Delay in Diesel Engines," *SAE paper*, No. 961123.

Schwarz, V. et al., 1999, "Analysis of Mixture Formation, Combustion and Pollutant Formation in HD Diesel Engines Using Modern Optical Diagnostics and Numerical Simulation," *SAE paper*, No. 1999-01-3647.